Recombination Line Spectroscopy : Measuring Temperature

Rob Bastin and Peter Storey, University College London

Introduction

A problem in the study of many planetary nebulae is the discrepancy between temperatures and abundances derived from collisionally excited lines and recombination lines.

- Temperature from collisionally excited lines larger than from the Balmer line/continuum ratio.
- Abundances from metal recombination lines larger than from collisionally excited lines.

Strong recombination line emission might arise from,

- Knots of cool ($\sim 10^3 K$) metal-rich material distributed throughout planetary nebulae[1]
- Regions of high dust concentration and possibly high temperature (several $10^4 K$)[2]

In the second scenario, recombination lines would be enhanced by high-temperature dielectronic recombination (HTDR). Current nebular recombination line theory does not incorporate this process, which occurs through high-n Rydberg states.

Unlike low-temperature dielectronic recombination, HTDR enhances recombination lines in the principal series of the recombined ion. We have studied the recombination lines of CII as an example. We address two questions.

1. How strongly does HTDR enhance recombination lines?
2. Can the low and high temperature scenarios be distinguished from spectroscopy of recombination lines? In other words, can we measure the temperature of the material emitting the recombination lines?

High Temperature Dielectronic Recombination : Theory

A collision between an ion X^+ and a continuum electron can lead to the formation of a doubly excited state above the lowest ionisation energy of X^+. There are two possible outcomes, autoionisation or dielectronic recombination.

$$X^+ + e^- \rightleftharpoons X^{**} \rightarrow X^{+*} + h\nu \tag{1}$$

The rate coefficient for dielectronic recombination is given by Seaton and Storey[3] as :

$$\alpha_d = \frac{\omega^{**}}{2\omega^+} S(T) \exp\left(\frac{-E(X^{**})}{kT}\right) \frac{\Gamma^A \Gamma^R}{\Gamma^A + \Gamma^R} \tag{2}$$

where $S(T) = (h^2/2\pi m kT)^{3/2}$, ω^{**}, ω^+ are statistical weights, $E(X^{**})$ is energy above the ionisation threshold, k is the Boltzmann constant, T is the electron temperature, Γ^A is the probability of autoionisation (s^-1), Γ^R is the probability of radiative decay (s^{-1}). h is the Planck constant and m is the electron mass.

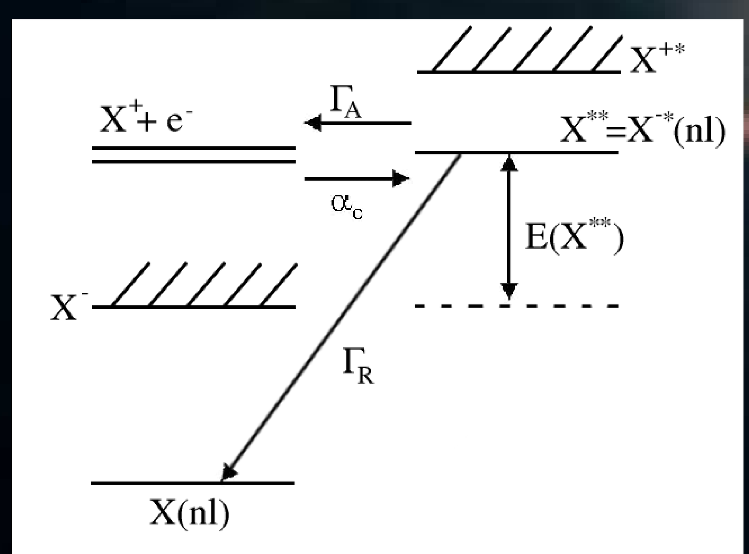

Figure 1 : Schematic of the three key processes in dielectronic recombination

Here X^+ is $C^{2+}[2s^2(^1S)]$, X^{**} is $C^+[2s2p(^1P^o)nl]$ and X^{+*} is $C^+[2s^2(^1S)nl]$

High Temperature Dielectronic Recombination : Method

We solve the C^+ level population problem in three stages.

1. Solve an n-resolved hydrogen-like problem (for all n)[4].
2. Solve an nl-resolved hydrogen-like problem[4].
3. Solve an nl-resolved C^+ problem[5].

Bound-bound and bound-free C^+ radiative data is computed using the R-matrix method of electron-ion scattering theory. Radiative and autoionisation probabilities for HTDR are computed using AUTOSTRUCTURE[6,7].

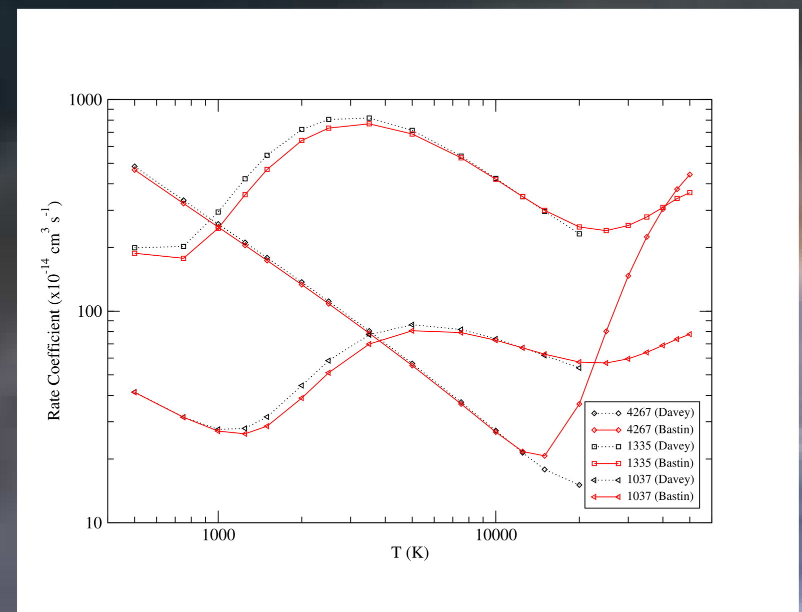

Figure 2 : Plot comparing Davey et al.[5] with this work for three strong recombination lines (density $10^4 cm^{-3}$).

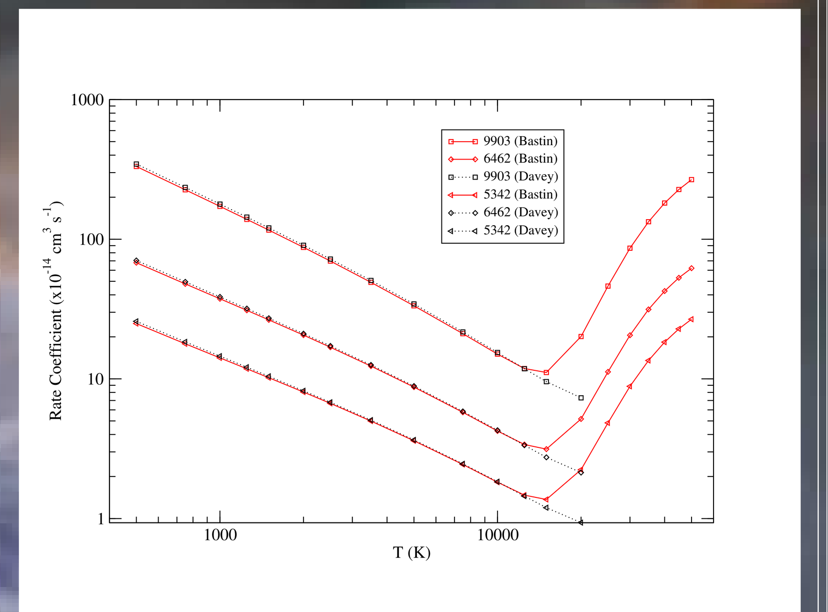

Figure 3 : Plot comparing Davey et al.[5] with this work for three optical recombination lines (density $10^4 cm^{-3}$).

With level populations, we can compute temperature and density dependent effective recombination coefficients. Some examples and a comparison with previous work is shown in table 1.

The main features are:

- Good low temperature agreement with Pequignot et al.[8] and Davey et al.[5].
- Clear contribution of HDTR for T$\geq$ 15000K.

With rate coefficients, we can generate theoretical line ratios for lines in ionised nebulae.

They may be temperature dependent, providing a measure of the electron temperature.

Transition	$\lambda[\mathring{A}]$	Case	Pequignot	Davey	This Work
$7g(^2G)$ - $4f(^2F^o)$	5342	A	-	0.184	0.182
$6g(^2G)$ - $4f(^2F^o)$	6462	A	-	0.429	0.424
$5g(^2G)$ - $4f(^2F^o)$	9903	A	1.621	1.545	1.506
$6f(^2F^o)$ - $4d(^2D)$	6151	A	-	0.166	0.165
$4f(^2F^o)$ - $3d(^2D)$	4267	A	2.795	2.727	2.684
$3d(^2D)$ - $3p(^2P^o)$	7235	A	0.065	0.079	0.078
$3d(^2D)$ - $3p(^2P^o)$	7235	B	5.184	5.587	5.561
$3p(^2P^o)$ - $3s(^2S)$	6580	A	0.329	0.620	0.611
$3p(^2P^o)$ - $3s(^2S)$	6580	B	1.444	3.288	3.236
$3p(^2P^o)$ - $2s2p^2(^2S)$	2841	A	0.606	0.622	0.654
$3p(^2P^o)$ - $2s2p^2(^2S)$	2841	B	3.301	2.658	3.464
$2s2p^2(^2D)$ - $2p(^2P^o)$	1335	A	3.450	42.39	42.03

Table 1 : Comparison of effective recombination coefficients (in 10^{-13} $cm^3 s^{-1}$) at a temperature of 10000K and density of $10^4 cm^{-3}$ from Pequignot et al.[8], Davey et al.[7] and this work

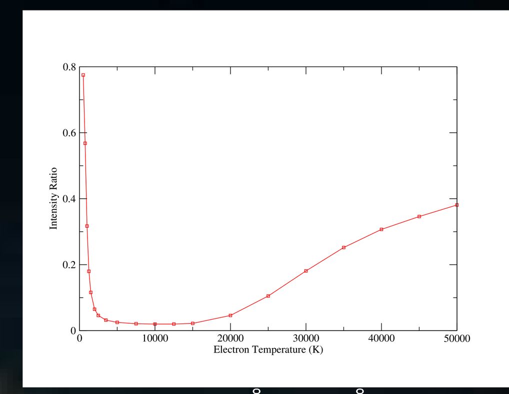

Figure 4 : 4267$\mathring{A}$/1335$\mathring{A}$ intensity ratio against electron temperature.

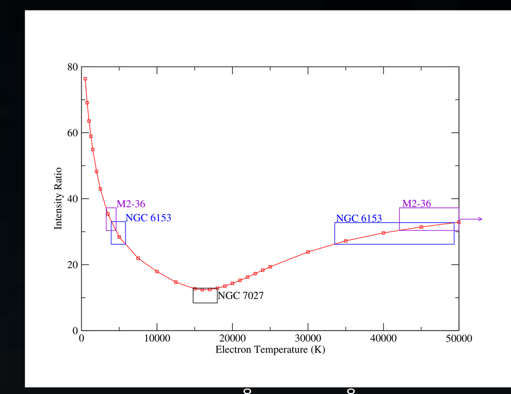

Figure 5 : 4267$\mathring{A}$/3920$\mathring{A}$ ratio, with observed ratios for three PNe (boxes show 2σ uncertainty).

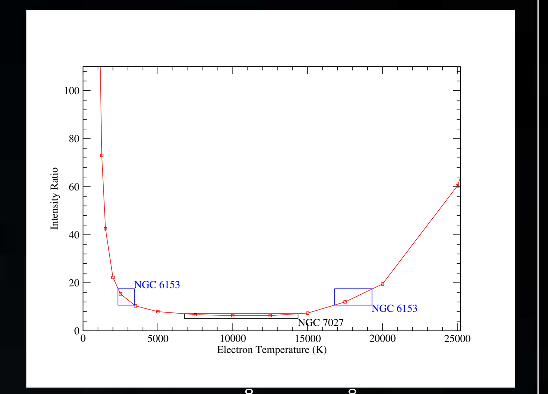

Figure 6 : 9903$\mathring{A}$/8793$\mathring{A}$ ratio, with observed ratios for two PNe (boxes show 2σ uncertainty).

Results

In Table 2 we show the intensities of various CII recombination lines relative to the λ4267 intensity, at three electron temperatures.

- Optical recombination lines are predominantly excited by radiative recombination until HTDR switches on at $T \geq 15000$ (Fig 3). The greatest sensitivity to temperature is found between the transitions with the largest differences in orbital angular momentum, l, e.g. $4s - 3p$; λ3920 vs. $4f - 3d$; λ4267 (see Fig 5).
- The two UV lines λ1036 and λ1335, along with the λ8800 are primarily excited through low-lying resonances and therefore show a strong variation with electron temperature at temperatures of a few thousand Kelvin (see Fig 6 for λ8800).

$\lambda[\mathring{A}]$	Trans.	Line Emissivities		
		1000K	10000K	30000K
UV:				
1036	2p-2s	0.440	11.014	1.582
1335	2p-2s	3.110	49.28	5.230
3920	4s-3p	0.015	0.055	0.040
Optical:				
4267	4f-3d	1.000	1.000	1.000
4802	8g-4f	0.024	0.031	0.028
5342	7g-4f	0.044	0.053	0.047
6151	6f-4d	0.027	0.043	0.038
6462	6g-4f	0.098	0.103	0.091
6580	3p-3s	0.448	0.769	0.607
IR:				
7234	3d-3p	0.912	1.203	1.082
8800	3d-3p*	0.002	0.036	0.002
9903	5g-4f	0.295	0.239	0.254
18516	6h-5g	0.102	0.070	0.082

Table 2 : Theoretical line emissivities relative to 3d-4f (4267$\mathring{A}$) at three temperatures.

Nebular Temperatures

Figs 5 and 6 compare theory and observation for three PNe.

NGC 7027 : Recombination line and forbidden line abundances are in broad agreement and the recombination line temperatures are also in broad agreement with the temperatures from forbidden lines.

NGC 6153[1] and M2-36[9] : Recombination line abundances are found to be much larger than forbidden line abundances, by a factor of ten in NGC 6153 and five in M2-36. Figs 5 and 6 show that the temperature of the recombination line emitting regions are markedly different from the collision line temperatures of $\sim$9000K for NGC 6153 and $\sim$8000K for M2-36.

Conclusion

With a careful choice of spectral lines, CII recombination lines can be used to measure the electron temperature of the emitting region. The good agreement between recombination line and collisionally excited line temperatures for NGC 7027 gives confidence in the method. PNe with large recombination/collisional abundance discrepancies have measured recombination line temperatures very different to collisional line temperatures, but we cannot conclusively distinguish between a low and a high temperature solution.

References : 1) X. W. Liu et al, MNRAS, 312, 585-628, 2000, 2) Stasinska and Szczerba, A & A, 379, 1024-1038, 2001, 3) Seaton and Storey, Atomic Processes and Applications, Chapt. 6, North Holland Pub. Co., 1976, 4) Hummer and Storey, MNRAS, 224, 801-820, 1987, 5) Davey et al, A & ASS, 142, 85-94, 2000, 6) K. A. Berrington, P. G. Burke et al., J.Phys.B v20 pp6379-97, 1987, 7) N. R. Badnell, J.Phys.B v32 pp5583-91, 1999, 8)Pequignot et al. A & A, 251, 680-688, 1991, 9) X. W. Liu et al., MNRAS, 327, 141-168, 2001

UCL
EPSRC Engineering and Physical Sciences Research Council

Background image courtesy of NASA/ESA/HEIC/AURA